Supporting Information: Rapid Structural, Kinetic and Immunochemical Analysis of Alpha-Synuclein Oligomers in Solution

William E. Arter[1,2,†], Catherine K. Xu[1,†], Marta Castellana-Cruz[1],
Therese W. Herling[1], Georg Krainer[1], Kadi L. Saar[1],
Janet R. Kumita,[1] Christopher M. Dobson & Tuomas P. J. Knowles[1,2,*]
[1]Department of Chemistry, University of Cambridge, Lensfield Rd, Cambridge, CB2 1EW UK
[2]Cavendish Laboratory, University of Cambridge, JJ Thomson Avenue, Cambridge, CB3 0HE, UK
[†]These authors contributed equally
[‡]Deceased September 2019
*Corresponding author. Email tpjk2@cam.ac.uk

Contents

1 Supplementary Methods

Expression and purification of α-synuclein

Wild-type α-synuclein was expressed and purified as previously described.[1] Briefly, Escherichia coli BL21 cells overexpressing α-synuclein were collected by centrifugation (20 min, 4000 rpm, 4 °C) in a JLA-8.1000 rotor in a Beckman Avanti J25 centrifuge (Beckman Coulter), resuspended in lysis buffer (10 mM Tris, 1 mM EDTA, protease inhibitor), and lysed by sonication on ice. Following centrifugation (JA-25.5 rotor, 20 min, 18,000 rpm, 4 °C), heat-sensitive proteins were precipitated out of the lysate supernatant by boiling, and subsequently removed by centrifugation (JA-25.5 rotor, 15 min, 18,000 rpm, 4 °C). DNA was precipitated out by incubation with streptomycin sulphate (10 mg/mL, 15 min, 4 °C), and removed by centrifugation. α-synuclein was precipitated out of the supernatant by the slow addition of ammonium sulphate (361 mg/mL) while stirring (30 min, 4 °C). The pellet containing α-synuclein was collected by centrifugation (JA-25.5 rotor, 15 min, 18,000 rpm, 4 °C) and resuspended in 25 mM Tris buffer, pH 7.4, 20 °C. Following dialysis to ensure complete buffer exchange, the protein was loaded onto a HiLoadTM 26/10 Q Sepharose high performance column (GE Healthcare), and eluted at ~350 mM NaCl, 20 °C with a salt gradient from 0 M to 1.5 M NaCl. Selected fractions were subsequently loaded onto a Superdex 75 26/60 (GE Healthcare) at 20 °C and eluted in PBS, pH 7.4, 20 °C. Protein concentration was determined by absorbance at 275 nm, using an extinction coefficient of 5600 M^{-1} cm^{-1}. The cysteine-containing variant (N122C) of α-synuclein was purified by the same protocol, with the addition of 3 mM DTT to all buffers.

Labelling of α-synuclein

α-Synuclein protein was fluorophore-labelled to enable visualisation by fluorescence microscopy.[2] In order to remove DTT, cysteine variants of α-synuclein were buffer exchanged into PBS or sodium phosphate buffer by use of P10 desalting columns packed with Sephadex G25 matrix (GE Healthcare). The protein was then incubated with an excess of Alexa488 or Alexa546 dyes with maleimide moieties (Thermofisher Scientific) (overnight, 4 °C on a rolling system) at a molar ratio of 1:1.5 (protein-to-dye). The labelling mixture was loaded onto a Superdex 200 16/600 (GE Healthcare) and eluted in PBS or 10 mM sodium phosphate pH 7.4 buffer at 20 °C, to separate the labelled protein from free dye. The concentration of the labelled protein was estimated by the absorbance of the fluorophores, assuming a 1:1 labelling stoichiometry (Alexa488: 72000 M^{-1} cm^{-1} at 495 nm, Alexa546: 112 000 M^{-1} cm^{-1} at 556 nm).

Preparation of stable α-synuclein oligomers

α-synuclein oligomers were prepared by the following procedure.[2] Monomeric α-synuclein was lyophilised in Milli-Q water and subsequently resuspended in PBS or 10 mM sodium phosphate buffer, both at pH 7.4, to give a final concentration of ca. 840 uM (12 mg/mL). The resulting solution was passed through a 0.22 uM cut-off filter before incubation at 38 °C for 20-24 h under quiescent conditions. Very small amounts of fibrillar species formed during this time were removed by ultracentrifugation for 1 h at 90000 rpm (Optima TLX Ultracentrifuge, Beckman Coulter, TLA-120.2 Beckman rotor, 288000 g). The excess monomeric protein and some small oligomers were then removed by multiple filtration steps using 100-kDa cut-off membranes. The final concentration of oligomers was estimated by the absorbance at 495 nm using a molar extinction coefficient of 72000 M^{-1} cm^{-1} for the Alexa488 labelled oligomers.

Procedure for generation and isolation of kinetic α-synuclein oligomers

Alexa488 labelled α-synuclein (N122C, 100 μM, 500-800 μL) was incubated in PBS buffer, pH 7.4, at 37 °C with 0.01% sodium azide, in a 1.5 mL Eppendorf tube with shaking at 200 rpm over 96 hours. 150 μL aliquots were withdrawn and centrifuged for 15 min at 21130 g, to pellet insoluble, fibrillar components of the reaction mixture. The supernatant, containing monomeric and oligomeric α-synuclein, was carefully removed and used immediately for FFE experiments. A small portion of the supernatant was retained for analysis of α-synuclein concentration by UV-vis absorption spectroscopy.

Microfluidic device fabrication

Devices were designed using AutoCAD software (Autodesk) and photolithographic masks printed on acetate transparencies (Micro Lithography Services). Polydimethylsiloxane (PDMS) devices were produced on SU-8 moulds fabricated *via* photolithographic processes as described elsewhere,[3,4] with UV exposure performed with custom-built LED-based apparatus.[5] Following development of the moulds, feature heights were verified by profilometer (Dektak, Bruker) and PDMS (Dow Corning, primer and base mixed in 1:10 ratio) applied and degassed before baking at 65 °C overnight. Devices were cut from the moulds and holes for tubing connection (0.75 mm) and electrode insertion (1.5 mm) were created with biopsy punches, the devices were cleaned by application of Scotch tape and sonication in IPA (5 min). After oven drying, devices were bonded to glass slides using an oxygen plasma. Before use, devices were rendered hydrophilic *via* prolonged exposure to oxygen plasma.[6]

μFFE device operation

Liquid-electrode microchip free-flow electrophoresis (μFFE) devices were operated as described previously.[7] Briefly, fluids were introduced to the device by PTFE tubing, 0.012"ID x 0.030"OD (Cole-Parmer) from glass syringes (Gas Tight, Hamilton) driven by syringe pumps (Cetoni neMESYS). μFFE experiments were conducted with auxiliary buffer, electrolyte, monomer reference and sample flow rates of 1200, 250, 140 and 10 μL h^{-1}, respectively, for 15× reduction in buffer salt concentration for samples in PBS buffer.

Potentials were applied by a programmable benchtop power supply (Elektro-Automatik EA-PS 9500-06) *via* bent syringe tips inserted into the electrolyte outlets. Device voltage efficiency was calibrated by comparison of current-voltage curves of the device operating under assay conditions and when filled with 3M KCl electrolyte. Efficiencies were found to be ≈20%, affording electric fields equivalent to 200-267 V cm^{-1} for potentials of 300–400 V.

Microfluidic experiments were conducted using an inverted fluorescence microscope (Zeiss AxioObserver D1), Alexa488, 546 and 647-labelled species were observed using appropriate filter sets (49002, 49004 and 49006, Chroma Technology) and camera (Evolve 512 CCD, Photometrics). Control experiments confirmed negligible spectral overlap between the filter sets employed.

Oligomer μFFE experiments

Alexa488-labelled oligomeric mixtures (4 μM monomer equivalent for stabilised oligomers) in either 10 mM sodium phosphate pH 7.4 or PBS buffer were mixed on-chip with Alexa546-labelled monomer (2 μM) in either 10 mM sodium phosphate pH 7.4 or pure water, respectively. For oligomeric samples in 10 mM sodium phosphate or PBS buffer, auxiliary buffer comprised of the same or 15X diluted PBS buffer, respectively, supplemented with 0.05% v/v Tween-20.

Following data acquisition, Alexa488 and Alexa546 fluorescence profiles were extracted by taking a line profile (100-pixel thick) perpendicular to the direction of flow using ImageJ software. The fluorescence profiles were superimposed and normalised to the maximum peak fluorescence of the Alexa546 monomer. This operation enabled visualisation and subsequent subtraction of the monomer-only component of the monomer+oligomer mixture visible in the 488 channel, and accounted for differences in monomer fluorescence intensity between the 488 and 546 channels which occur due to differences in protein concentration and in the characteristics of the fluorophores. This process resulted in almost identical 488 and 546 fluorescence profiles for the monomer portion of the combined electropherogram (Fig1(d, e), main text).

Subtraction of the normalised Alexa546 from the Alexa488 profile afforded profiles due to oligomeric aggregates alone. For quantification of oligomers formed transiently during αS aggregation, the

relative peak integrals of oligomeric and monomer populations were compared to the known monomer concentration and degree of sample loss during desalting (see below) to calculate the oligomer concentration.

Aptamer-oligomer μFFE experiments

Wild-type αS (100 μM) was mixed with Alexa647-labelled aptamer (2 μM, Integrated DNA Technologies, sequence is provided in the Supporting Information) in PBS buffer and underwent aggregation by rapid stirring.[8] 150 uL aliquots were withdrawn every hour and fibrillar material was removed by centrifugation. The sample then underwent desalting-μFFE analysis as described above.

Analytical ultra-centrifugation

Sedimentation velocity measurements[9] were carried out at 20 °C, 43000 rpm (136680 g), using a Beckman Coulter Optima XL-1 analytical ultracentrifuge equipped with UV-visible absorbance optics and an AN50-Ti rotor. The sedimentation coefficient distributions, corrected to standard conditions by using the SEDNTERP programme, were calculated via least-squares boundary modelling of sedimentation velocity data using the c(s) and ls-g*(s) methods, as implemented in the SEDFIT programme.[10]

2 Desalting μFFE

To increase the applicability of our method towards the analysis of oligomeric samples in general, including under physiological conditions, we sought to remove the constraints regarding buffer type that are a feature of other electrophoresis experiments. μFFE fractionation requires low-salt conditions (e.g. typically < 20 mM NaCl), often facilitated through the use of non-physiological buffering agents,[11] in order to minimise ionic conduction which can otherwise severely limit the electric field that can be induced across the electrophoresis chamber. This is problematic for the analysis of samples in high-salt, physiological buffers such as PBS, and is particularly relevant in the context of protein aggregation given the effect of solution conditions on oligomer stability and formation-dissociation kinetics.[12,13]

A desalting module was incorporated into the μFFE device, upstream of the electrophoresis chamber, to rapidly decrease the salt concentration on chip to enable electrophoretic analysis (Figure S1).

The desalting module functions by exploiting the relatively slow rate of diffusion for high molecular weight proteins and protein oligomers in comparison to that of salt ions. Sample solutions undergo diffusional mixing with salt-free water during passage through the desalting module, salts diffuse the full width of the microfluidic channel and are diluted according to the relative flow rates of sample and

diluent, whilst proteins only partially diffuse and remain at higher concentration before passage into the electrophoresis chamber. The protein is then re-collected on-chip, before passing into the electrophoresis chamber of the device for μFFE analysis. Although a proportion of the sample is lost using this technique, this effect is minimised for species with slow diffusion such as the large oligomeric complexes of interest here. The degree of sample loss is shown in Figure S1(c, d), with 47% of monomer (r = 3 nm) retained for electrophoresis, increasing to 65–75% for oligomers of r = 6.4–10 nm.[2] Ionic strength can be readily reduced by up to 20×, bringing samples initially in PBS into suitable operating conditions for effective μFFE. Importantly, this desalting process occurs quickly, with the initial desalting step and total time on chip being ~1.8 and 3.5 seconds, respectively. Therefore, it is predicted that desalting will not significantly affect oligomer structure over the assay timescale, which is significant since solution conditions are known to influence aggregate stability.[12] In addition, the monomer protein reference can be co-injected with the salt-free diluent, minimising the time for potential interactions between reference and analyte.

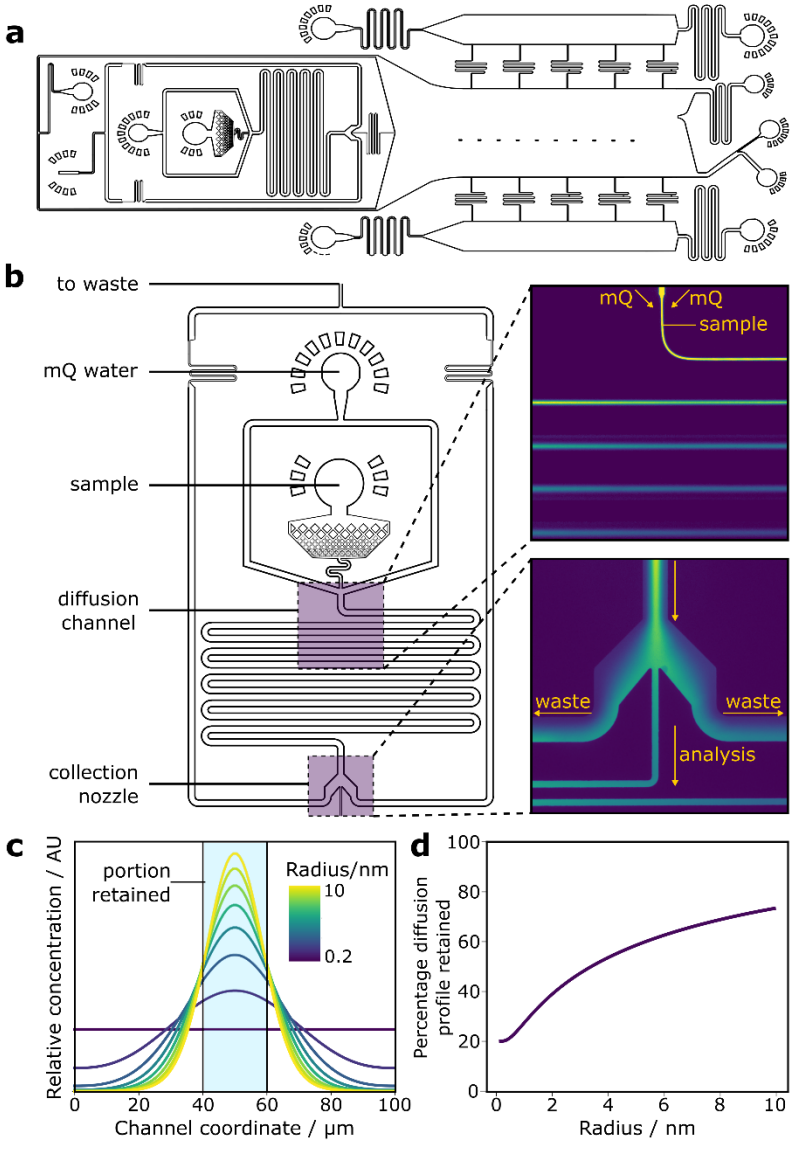

C

Figure S1 μFFE device with in-line desalting module. (a) Schematic of desalting-μFFE device design. (b) Enlarged schematic of the desalting module. (Inset, upper) Fluorescence micrograph of αS monomer flowing into the desalting-diffusion region. (Inset, lower) Fluorescence micrograph of desalting 'nozzle', showing central portion of αS monomer diffusion profile being selected for downstream μFFE analysis. (c) Schematic showing region of diffusion profiles for r = 0.2 nm (Na^+ ions) to r = 10 nm (approximate size of αS oligomers). (d) Plot of percentage of protein retained for downstream analysis as a function of hydrodynamic radius.

3 Validation of two-colour approach

For the dual-colour approach described here, it is necessary that both Alexa488 and Alexa546 labelled αS possess the same electrophoretic properties. Since both dyes possess the same charge (−2 *e*) and a similar structure, the difference between the labelling variants was expected to be minimal. To verify this prediction, the electrophoretic mobilities of monomeric Alexa488 and Alexa546 labelled αS were quantified using previously described methods (Figure S2).[7] From microscopy images of electrophoretic deflection at the two label wavelengths, no difference could be observed between the two labelling variants (Figure S2(b, c)). To assess this finding quantitatively, the electrophoretic mobilities of the variants were found by plotting the electrophoretic drift velocity as a function of applied electric field. From the linear relationship obtained, it was clear that the measured electrophoretic mobility of $\mu = -1.43 \pm 0.11 \times 10^{-8}\ m^2\ V^{-1}\ s^{-1}$ was the same for both fluorophores within experimental error.

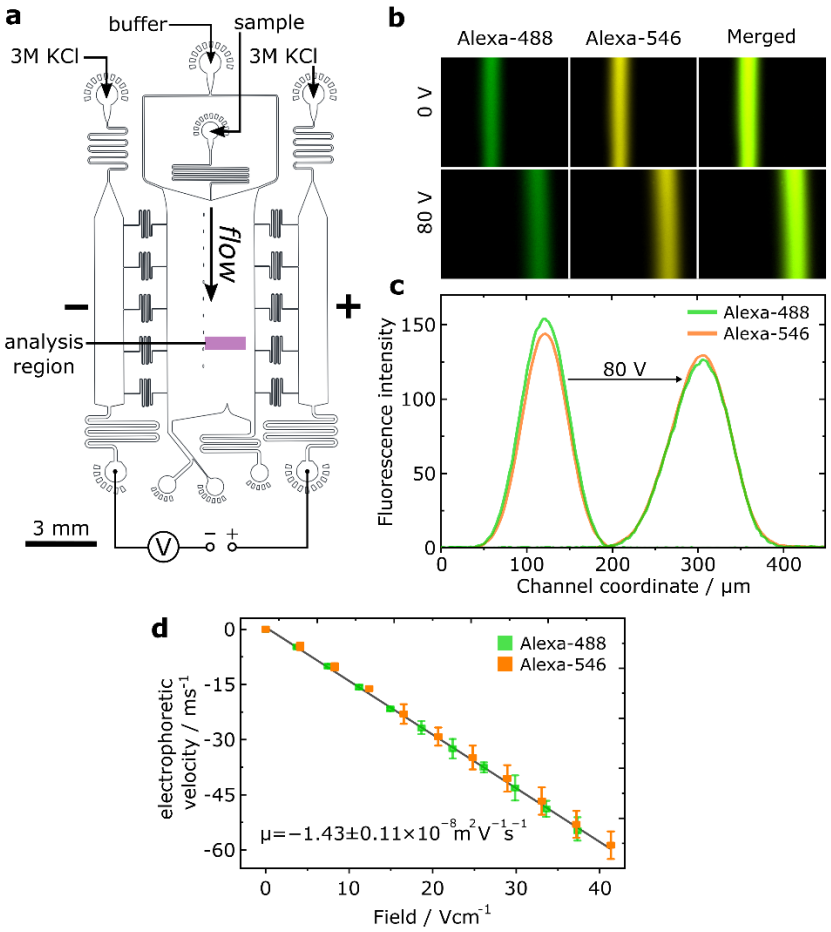

Figure S2 Quantitative FFE of monomeric αS. (a) Design with annotated fluid inlets for the microfluidic FFE device used for quantification of monomeric αS and oligomeric αS in low-salt buffer. (b) Microscopy images of Alexa488, Alexa546 and merged fluorescence of labelled αS monomer, mixed in the same sample and imaged using orthogonal excitation and emission filters, at 0 V and 80 V. (c) Superimposed electropherograms of Alexa488 and Alexa546 labelled αS at 0 V and 80 V corresponding to images shown in (b). (d) Scatter plot and linear fit of Alexa488 and Alexa546 electrophoretic velocities as a function of applied field. Both labelling variants display the same electrophoretic mobility within experimental error.

4 Resolution in µFFE

To account for the finite resolution of the electrophoresis technique, we describe electrophoresis profiles in terms of 'apparent mobility'. Importantly, the mobilities of discrete electropherograms peaks are reported accurately in terms of their absolute value, but there exists an inherent uncertainty for electropherogram positions between intensity maxima. This uncertainty is given by the width of the sample beam under electrophoresis, the variance of which is approximated by:[14]

$$\sigma_{total}^2 = \sigma_{inj}^2 + \sigma_D^2 + \sigma_{HD}^2 = \frac{w_{inj}^2}{12} = \frac{2DL}{\nu} + \frac{hh^2d^2\nu}{105DL}$$

where σ_{inj}^2, σ_D^2 and σ_{HD}^2 describe the injection width, diffusional and hydrodynamic contributions to the total beam width. w_{inj} is the width of the sample injection stream, and v, D, L, d, and h are the linear flow velocity, diffusion coefficient, channel length beam deflection and channel height, respectively. For nominal oligomer and monomer radii of 6.4 nm and 3 nm,[15,16] values of $\sigma_{total} =$ 176 µm and 80 µm were calculated for the flow conditions and device geometry used here. Although these values correspond to 28% and 25% of the respective total deflection for oligomer and monomer, an important factor to note is that this band-broadening effect does not prohibit the observation of discrete peaks in oligomer electrophoresis profiles. Thus, the finite resolution of µFFE does not preclude observation and analysis of oligomer heterogeneity.

5 ζ-potential calculations

ζ-potentials are typically calculated for colloidal systems where $\kappa r \gg 1$ using the Smoluchowski relation $\mu = \frac{\epsilon_0 \epsilon_r \zeta}{\eta}$ where κ is the inverse Debye length and r is the particle radius. However, using the most common oligomer radius of $r_o = 6.4$ nm as determined by AUC,[2,15] and since $\kappa = 0.52$ nm^{-1} in our experiment (10 mM NaPi), $\kappa r \approx 3.3$ and the Smoluchowski model is therefore an unsuitable model for our data. Instead, the Henry equation:[17]

$$\zeta = \frac{3\mu\eta}{2\epsilon_0 \epsilon_r f_H(\kappa a)}$$

provides a better approximation, where f_H is the Henry function, approximated as:[17]

$$f_H(\kappa a) = 1 + \frac{1}{2(1+\delta)^3}$$

$$\delta = \frac{5}{2\kappa a(1 + 2e^{-\kappa a})}$$

from these equations, values of $\delta = 0.7$ and $f_H(\kappa a) = 1.1$ were obtained for $r = 6.4$ nm. Thus, a value of $\zeta = -42.6 \pm 4.1$ mV was obtained for the largest population of oligomers where $\mu = -2.49 \pm 0.16 \times 10^{-8}$ m^2 V^{-1} (main text, Figure 1(f)).

6 Additional analyses of stabilised oligomers

Figure S3 shows additional data for µFFE and AUC analysis of oligomer heterogeneity, from oligmomeric mixtures synthesised in either 10 mM sodium phosphate or PBS buffer. For the NaPi sample, a different oligomer profile is observed compared to the analysis described in the main text, due to differences between samples caused by small variances in oligomer preparation. Importantly, the AUC and µFFE data is self-consistent within each sample dataset, confirming the efficacy of our approach.

In the case of the PBS samples, clear separation between the oligomer and monomer peaks demonstrates effective sample preparation by the microfluidic desalting unit. By comparing the data between the NaPi and PBS-buffered samples, a greater concentration of monomeric αS is present in the lower-salt conditions. This is due to a greater degree of sample dissociation occurring under low ionic strength during the time between oligomer preparation and measurement (2–4 h).[12] Notably, the monomeric fraction is minimal in comparison to the oligomer peak observed in the μFFE data for PBS-buffered oligomers. This implies that no appreciable dissociation of oligomers occurs during the timescale of the μFFE experiment.

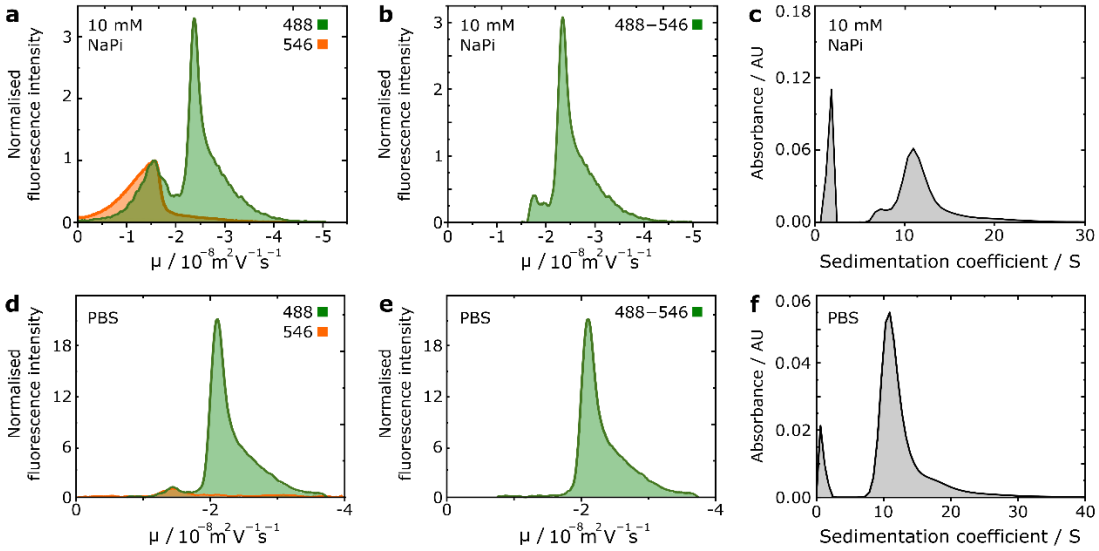

Figure S3 Additional μFFE and AUC data for synthetic oligomers. (a) Superimposed electropherograms for monomer-normalised Alexa546 labelled monomer and Alexa488 labelled oligomer sample in 10 mM NaPi buffer. (b) Electropherogram corresponding to only the oligomeric fraction of an oligomer sample in 10 mM NaPi buffer. (c) AUC data for the same oligomer sample as in (a) and (b), the peak at S ≈ 2 is due to monomeric protein. (d) Superimposed electropherograms for μFFE of monomer-normalised Alexa546 labelled monomer and Alexa488 labelled oligomer sample desalted on chip from PBS buffer. (e) Electropherogram corresponding to only the oligomeric fraction of an oligomer sample desalted on chip from PBS buffer. (f) AUC data for the same oligomer sample as in (d) and (e), the peak at S ≈ 2 is due to monomeric protein.

7 Analytical ultracentrifugation

To obtain an independent measure of structural heterogeneity, AUC experiments were conducted using the same two samples of stable αS oligomers. AUC quantifies the sedimentation coefficient (s) of particles, defined as the ratio of a particle's sedimentation velocity to the applied acceleration that causes the sedimentation. s is given by:

$$s = \frac{m}{6\pi\eta r}$$

where m and r are the mass and radius of the particle. For oligomers, the mass of particles will share a linear relationship with the degree of oligomerisation n_m, which is in turn related to the net charge and electrophoretic mobility according to:

$$\mu_o \propto \frac{q_o}{r_o} \propto \frac{n_m^{\nu}}{r_o}$$

$$n_m \approx \frac{V_o}{V_m} = \frac{r_o^3}{r_m^3}$$

$$r_o = r_m n_m^{\frac{1}{3}}$$

$$\mu_o \propto \frac{n_m^{\nu}}{r_m n_m^{\frac{1}{3}}} \propto \frac{n_m^{\nu*}}{r_m}$$

Therefore, the sedimentation coefficient may scale with oligomer size in a similar manner to electrophoretic mobility according to:

$$s_o \propto \frac{m_o}{r_o} \propto \frac{n_m}{r_o}$$

$$\mu_o \propto s_o^{\nu*}$$

where s_o and m_o are the sedimentation coefficient and mass of an oligomer of n_m monomer units, respectively. Therefore, similar observations of oligomer heterogeneity are expected between µFFE and AUC, though these measurements are not directly proportional due to the scaling exponent $0 < \nu < 1$, that links net oligomer charge to n_m.

Oligomer hydrodynamic radii were approximated from AUC data by calculation of oligomer mass as a function of oligomer size, assuming spherical oligomers and protein density[18] $\rho = 1.35$ gcm^{-1} according to:

$$S = 10^{-13}\, s = \frac{V_o \rho}{6\pi\eta r_o}$$

8 Biophysical characterisation of labelled oligomers

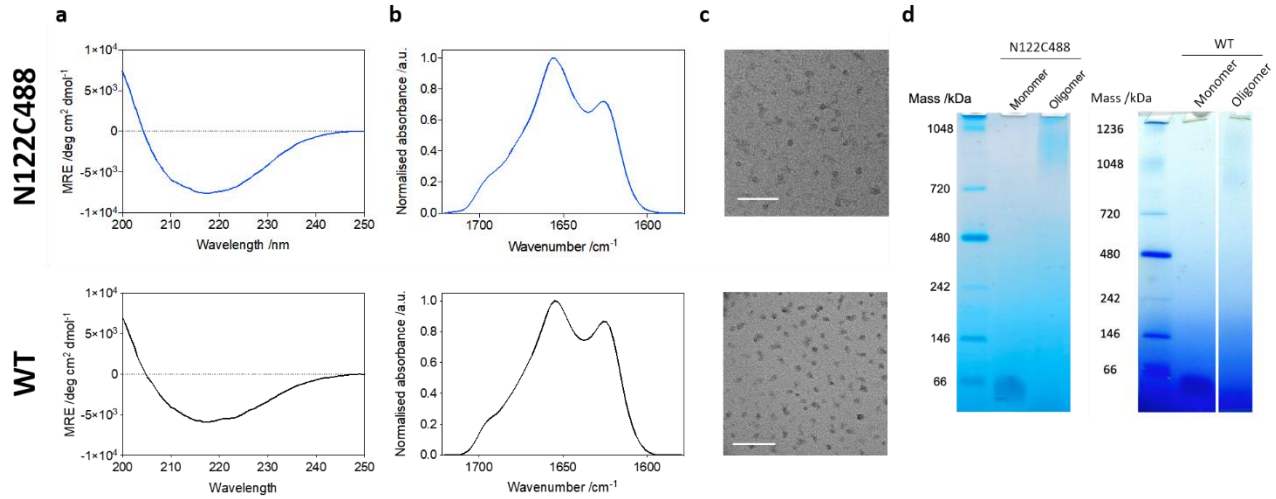

Figure S4 Biophysical characterisation of Alexa488-labelled and wild-type stable αS oligomers. (a) Representative circular dichroism (CD) spectra of oligomers formed of Alexa488 labelled N122C (upper) and wild-type (lower) alpha-synuclein. (b) Representative Fourier-transform infra-red spectroscopy (FTIR) spectra of oligomers formed of Alexa488 labelled N122C (upper) and wild-type (lower) alpha-synuclein, showing the expected antiparallel β-sheet structural content.[2] (c) Transmission electron microscope (TEM) image of oligomers formed of Alexa488 labelled N122C (upper) and wild-type (lower) alpha-synuclein (scale bar = 100 nm). (d) Gel electrophoresis of Alexa488 labelled N122C monomer and oligomer (left) and wild-type (WT) αS monomer and oligomer (right). The large apparent mass of monomeric αS (true mass ≈ 14 kDa) is ascribed to the intrinsically disordered properties of αS, as opposed to the globular proteins of the marker ladder. Further comparison, including atomic force microscopy (AFM) analysis between wild-type and labelled αS oligomer can be found in previously published work.[2]

9 Aggregation of Alexa488-labelled αS

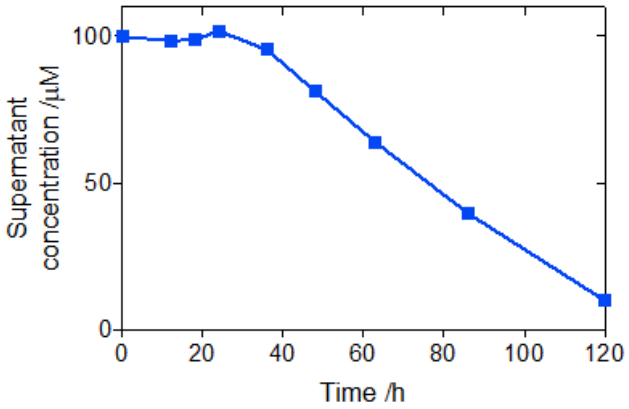

Figure 5 Aggregation kinetics of Alexa488-labelled αS under shaking (200 rpm) at 37 °C, PBS pH 7.4. Fibrils were removed by centrifugation (21,130 rcf, 10 min, 25 °C) and the supernatant concentration quantified by UV-Vis spectroscopy at 495 nm.

10 Aptamer-oligomer interactions

The aptamer used here (Table S1) is known to be strongly selective for oligomers, but also weakly binds fibrillar αS.[19] To exclude the possibility of the lower-mobility band observed in the 4.25 h αS aggregration timepoint being due to aptamer binding to erroneously retained fibrillar material, μFFE was conducted with a sample mixture comprising aptamer and fibrillar αS (Figure S6(a, b)). A clear difference in electrophoretic mobility and electropherogram profile was observed for the aptamer band, in comparison to both the t = 0 and t = 4.25 h timepoints. This indicates that fibrillar material may also be detectable by μFFE, as suggested previously,[7] and that the band observed at t = 4.5 h can be assigned to aptamer-oligomer binding.

Samples of αS fibrils were prepared as described previously.[2] Briefly, monomeric αS at 70 μM in PBS buffer pH 7.4, 0.01% NaN_3, was incubated under constant agitation (37 °C, 200 rpm) for 4–6 days. After this time, each sample was centrifuged (15 min at 13200 rpm) and the fibrillar pellet washed twice with PBS before being resuspended into the appropriate volume of PBS. The final concentration of fibrils, that was typically ca. 100 μM in each sample, was estimated by measuring the absorbance at 275 nm using a molar extinction coefficient of 5600 M^{-1} cm^{-1} after disaggregating an aliquot in the presence of 4M guanidinium chloride. To reduce their size to ≈100 nm to prevent blockage of device channels, fibrils were sonicated (20s, 10% power, 30% cycle) prior to use. Aptamer-fibril μFFE was conducted in PBS buffer pH 7.4, with aptamer and fibril (monomer equivalent) concentrations of 2 μM and 100 μM, respectively.

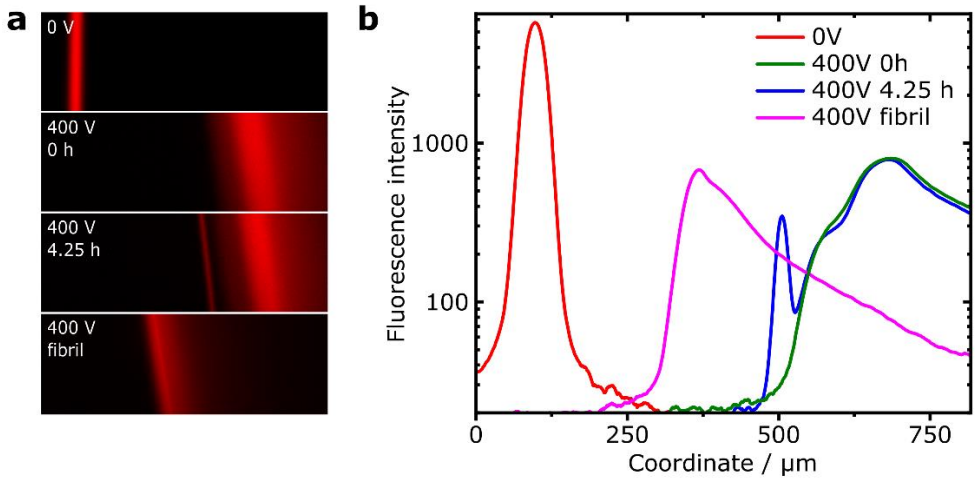

Figure S6 (a, upper three panels) Microscopy images of aptamer fluorescence during µFFE, from aptamer mixed into an aggregation reaction of wild-type αS, as in the main text. (Bottom panel) µFFE of an aptamer-fibril mixture, using sonicated fibrils of wild-type αS. (b) Electrophoresis profiles of aptamer µFFE, as in main text, with addition of profile for aptamer-fibril mixture.

DNA oligonucleotide	**Sequence**
αS oligomer-selective aptamer	5’-(Alexa647)-ATTTGCCTGTGGTGTTGGGGCGGGTGCG-3’

Table S1 DNA sequence for aptamer selective for αS oligomers. Aptameric sequence T-SO508 is underlined.[19] Additional four bases were added to provide spacer between aptameric region and fluorophore.

References

1. Hoyer, W. *et al.* Dependence of α-Synuclein Aggregate Morphology on Solution Conditions. *J. Mol. Biol.* **322**, 383–393 (2002).
2. Chen, S. W. *et al.* Structural characterization of toxic oligomers that are kinetically trapped during α-synuclein fibril formation. *Proc. Natl. Acad. Sci. U. S. A.* **112**, E1994-2003 (2015).
3. Mazutis, L. *et al.* Single-Cell Analysis and Sorting Using Droplet-Based Microfluidics. *Nat. Protoc.* **8**, 870–891 (2013).
4. McDonald, J. C. *et al.* Fabrication of Microfluidic Systems in Poly(dimethylsiloxane). *Electrophoresis* **21**, 27–40 (2000).
5. Challa, P. K., Kartanas, T., Charmet, J. & Knowles, T. P. J. Microfluidic Devices Fabricated Using Fast Wafer-Scale LED-Lithography Patterning. *Biomicrofluidics* **11**, 014113 (2017).
6. Tan, S. H., Nguyen, N.-T., Chua, Y. C. & Kang, T. G. Oxygen Plasma Treatment for Reducing Hydrophobicity of a Sealed Polydimethylsiloxane Microchannel. *Biomicrofluidics* **4**, 32204 (2010).
7. Saar, K. L. *et al.* On Chip Label Free Protein Analysis with Downstream Electrodes for Direct Removal of Electrolysis Products. *Lab Chip* **18**, 162–170 (2018).
8. Buell, A. K. *et al.* Solution conditions determine the relative importance of nucleation and growth processes in α-synuclein aggregation. *Proc. Natl. Acad. Sci. U. S. A.* **111**, 7671–7676 (2014).
9. Harding, S. E., Rowe, A. J. & Horton, J. C. *Analytical Ultracentrifugation in Biochemistry and Polymer Science*. (1992).
10. Schuck, P. www.analyticalultracentrifugation.com/default.htm.
11. Turgeon, R. T., Fonslow, B. R., Jing, M. & Bowser, M. T. Measuring Aptamer Equilbria Using Gradient Micro Free Flow Electrophoresis. *Anal. Chem.* **82**, 3636–3641 (2010).
12. Horrocks, M. H. *et al.* Fast Flow Microfluidics and Single-Molecule Fluorescence for the Rapid Characterization of α-Synuclein Oligomers. *Anal. Chem.* **87**, 8818–8826 (2015).
13. Kjaergaard, M. *et al.* Oligomer Diversity during the Aggregation of the Repeat Region of Tau. *ACS Chem. Neurosci.* **9**, 3060–3071 (2018).
14. Fonslow, B. R. & Bowser, M. T. Optimizing band width and resolution in micro-free flow electrophoresis. *Anal. Chem.* **78**, 8236–8244 (2006).
15. Andreasen, M., Lorenzen, N. & Otzen, D. Interactions between misfolded protein oligomers and membranes: A central topic in neurodegenerative diseases? *Biochim. Biophys. Acta - Biomembr.* **1848**, 1897–1907 (2015).
16. Yates, E. V *et al.* Latent analysis of unmodified biomolecules and their complexes in solution with attomole detection sensitivity. *Nat. Chem.* **7**, 802–809 (2015).
17. Doane, T. L., Chuang, C.-H., Hill, R. J. & Burda, C. Nanoparticle ζ-Potentials. *Acc. Chem. Res.* **45**, 317–326 (2011).

18. Fischer, H., Polikarpov, I. & Craievich, A. F. Average protein density is a molecular-weight-dependent function. *Protein Sci.* **13**, 2825–2828 (2004).
19. Tsukakoshi, K., Abe, K., Sode, K. & Ikebukuro, K. Selection of DNA Aptamers That Recognize α-Synuclein Oligomers Using a Competitive Screening Method. *Anal. Chem.* **84**, 5542–5547 (2012).